School of Physics

Masters Project
Physics

The Spread of Neolithic Farming

Markus Signitzer
March 2006

Abstract

This project tries to model the competing processes involved in the migration of Neolithic farming techniques: The displacement of Mesolithic hunter-gatherers by Neolithic farmers and the adoption of farming by hunter-gatherers. The used model extends the "wave of advance" - model originally introduced by Fisher [1] to describe the spread of advantaged genes in a population. The project investigates the suitability of computer simulations based on physical principles (Diffusion) to scientific areas outside physics, by comparing the simulation results with archeological, linguistic and genetic evidence.

Declaration

I declare that this project and report are my own work.

Signature: Date:

Supervisor: Dr. Graeme Ackland

Contents

1 Introduction **3**
1.1 A little overview of human history 3
1.2 The history of models and simulations 6

2 Method and Implementation **8**
2.1 Finding a solution to the Fisher Equation 8
2.2 Cohen's model 8
2.3 Extension to three populations and modifications 11
2.4 Software Implementation 13

3 Results & Discussion **16**
3.1 The Test Area 16
3.2 Europe 19
3.3 India 24
3.4 South Africa 27

4 Conclusion **30**

5 Acknowledgments **30**

A Appendices **33**
A.1 Finding a solution for the Fisher Equation 33
A.2 Solving the Diffusive Equation - Divergence of Fluxes 37
A.3 How to use the software 39
A.4 Source Code 39

1 Introduction

The transition from hunter gathering to early forms of agriculture in the Neolithic[1] was a fundamental event which put in place the foundation for human civilization. This project tries to show that a model based on a physical principle (Diffusion) can be used to model and visualize events and interactions outside the field of classical physics by applying it to the spread of Neolithic farming. Although this report will focus on the spread of farming, it is important to stress that the model can be easily applied to more general scenarios like the spread of an advantageous gene in a population or the usage of a tool or technology.

The project builds on a model from Cohen [13] which has its foundations in the "wave of advance" model originally introduced by Fisher [1] to model the advance of advantageous genes in a population. The simulation will include three different populations, the Mesolithic[2] hunter-gatherers, the Neolithic farmers and converts i.e. hunters and gatherers who have learned to farm. We will focus on four different scenarios. A generic test area to visualize the wave of advance and to test the model parameters, and three real world scenarios. The spread of farming into Europe and India and the special case of South Africa where the introduction of new crops by European farmers allowed the existing tropical farmers to expand further south.

The striking fact of this farming expansion is not only that it lay the foundation for the first civilizations, but also that we might still be able to observe some of its side effects in modern Europe. Scholars [10][11] think that it might be responsible for genetic and linguistic barriers observed in Europe. The great majority of European languages belong to the Indo-European family with five exceptions, namely Hungarian, Finnish, Lapp and Estonian which all belong to the Uralic language family and Basque, which can not be categorized. The presence of the Uralic family can be explained via invasions from the east, where the last one took place around 800 A.D when the Magyars conquered Hungary. The theory about the origin of Basque gos back all they way to the Neolithic expansion stating that the Basque are descendants of the hunter-gatherers living in Europe during the time of the spread of Neolithic farming. But before we go any deeper let us first set the scene.

1.1 A little overview of human history

Human history starts about 2 million years ago, with *homo habilis* probably being the first human species. Modern human i.e. *homo sapiens* (latin for *wise man*) history starts about 200,000 years ago or even earlier somewhere in Africa. The so far oldest remains identifiable as *homo sapiens* are three skulls found in Ethiopia in 2003, named *Hetro Skulls* [2]. They can be carbon dated to be between 155,000 and 160,000 years old. Since then, our ancestors set out and conquered the rest of the world in what is called the "Out of Africa" [3, 4] theory. See *Figure*[3] *1.*

[1] The Neolithic or younger Stone Age was about 10,000 years ago

[2] The Mesolithic or middle Stone Age is the period between the last glacial maximum and the start of the Neolithic

[3] *Figure 1 from: www.svf.uib.no/sfu/blombos/ Mod_H_The_Debate/images/cavali-sforza-map.jpg*

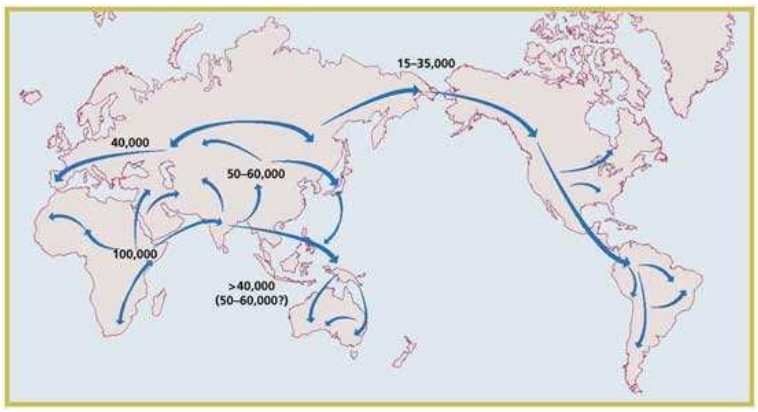

Figure 1: Migration of *homo sapiens* out of Africa

During their expansion, they successfully competed with other, sometimes older, human species for example the *homo neanderthalensis* or simply the Neanderthals. Although this might seem an exiting fact, modern human history remained rather boring for the next 150,000 years. Begging pardon to historians and archeologists who might object, but it seems that while living in small hunter-gatherer communities, the main achievements of that time where toolmaking, burial rites in connection with religion and simple art like painting and jewelry. But things changed dramatically about 10,000 years ago when farming was invented. Farming suddenly allowed a very different lifestyle compared to hunting and gathering. People could settle down, had a more reliable food source which sustained larger populations and also more free time to think about things. It was really the dawn of civilization because in its wake followed the first cities and the early empires. Farming arose as an independent development in several parts of the world [5]:

- There were three small center regions:

Region:	**Dominant Plants:**	**Date:**
Southwest Asia	wheat, barley	8500 B.C.
South China	foxtail millet, rice	7500 B.C.
Mesoamerica	maize, beans	3500 B.C.

This table is reproduced from *Table 5.1* in [6]

- Additionally, there existed three larger areas in the tropics of which the starting times are not so well known. The areas are the sub-Saharian regions in Africa, the Andes mountain range in South America and the islands of South East Asia.

The region in Southwest Asia which was most important for Europe's development is also know as the *Fertile Crescent*. It spawns in a half moon shape from south Israel over the Euphrates and Tigris river valley to the north coast of the Persian Gulf. See *Figure*[4] *2*. One might argue that this region, with the exception of the river valleys, is no

[4] *Figure* 2 from: http://oi.uchicago.edu/OI/MUS/GALLERY/EAST/New_East_Gallery.html

Figure 2: The fertile crescent.

longer very fertile today. However one has to keep in mind that 10,000 B.P. had a very different climate. It was the end of the last ice age which had its glacial maximum about 20,000 years ago. The glaciers were retreating, although Scotland and the Scandinavian countries were still partly covered in ice, and the sea level slowly rose about 45m to its current level, see *Figure*[5] *3*. An interesting side effect of this sea level rise is a catastrophe

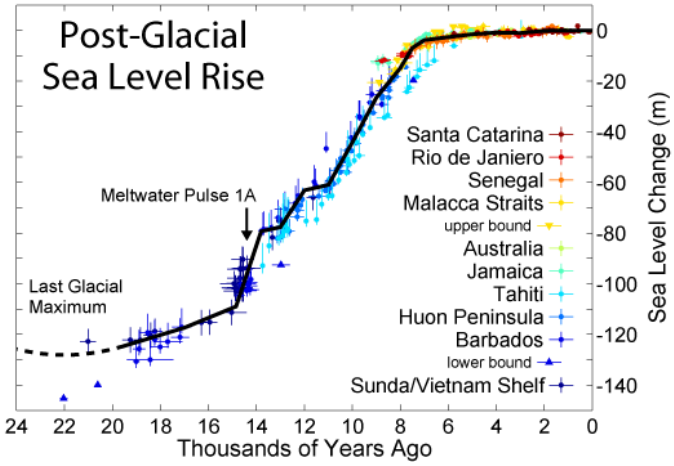

Figure 3: Sea level rise after the last ice age.

which might have served as a blueprint for the flood described in the Bible and could well have had an influence on the spread of farming, see section 3.2 for a more detailed discussion. Just how different the climate was during this time is illustrated well by cave paintings in the Sahara region [7]. These indicate that the Sahara was fertile and humid

[5] *Figure 3* from: http://en.wikipedia.org/wiki/Image:Post-Glacial_Sea_Level.png

from 10,000 to 5000 B.C., an arid steppe from 5000 to 3000 B.C. and a desert since then.

Let us again focus on the Fertile Crescent. Hand in hand with farming technology began the appearance of the first larger settlements. The most famous, or definitely most studied, is Jericho. Archaeological excavations indicate [9] that the first farmers settled on the banks of the Jordan river as early as 9600 B.C. Within a few hundred years Jericho had more than seventy houses and probably a population of more than a thousand people. It seems that across the ages, Jericho was almost constantly inhabited, making it probably the oldest town of the world. As farming started to spread from the Fertile Crescent by means of technology transfer as well as by migrating farmers, civilization followed in its wake, creating quite astonishing settlements like the city of Çatal Höyük [7] [9]. Situated in the central Anatolian Plain, this Neolithic city is unique with its beehive type clustered houses and with an average population of 5000 to 8000 people. It was founded around 6800 B.C. and remained occupied until 5400 B.C.
The rate at which farming spread from the Fertile Crescent was rather slow with about 1 km per year. The archaeological evidence for this rate of advance comes from excavations all over Europe where archaeologists link the arrival of farming with the arrival of pottery. However, this is only true for sites further west than Greece and Turkey, as pottery seems to have originated in the Sahara and then caught up with farming in Turkey or Greece [10]. By about 4000 B.C. farming had spread all over Europe reaching as far as Scotland. The Neolithic Transition had come to an end after almost 5000 years.

1.2 The history of models and simulations

This section tries to summarize the efforts of simulating the spread of Neolithic farming within the scientific community.

In 1936 the British geneticist R.A. Fisher [1] introduced the "wave of advance" model to predict the spread of an advantageous gene.
The ecologist J.G. Skellam used the model in 1948 to predict the spread of a population in two dimensions. In 1971 Ammerman and Cavalli-Sforza estimated the rate at which farming spread, using archaeological evidence, to be 1 km per year [15]. They were also the first to apply the "wave of advance"-model to the spread of Neolithic farming. It was introduced first in a paper [14] in 1973 and in more detail in their book "The Neolithic Transition and the genetics of populations in Europe" [12] in 1984 where they also include the results of a first computer simulation.

M.H. Cohen published a paper [13] in 1992 where he generalized the wave of advance model by introducing spatial inhomogeneity in the environment and complex contact interactions between different populations. However, he only suggests how the model should be expanded to three populations (i.e. Neolithic farmers, hunter-gatherers and converts) and did not include them in his paper. The most important innovation in his model is the introduction of *subsistence boundaries*. Compared to the obvious boundaries like coast lines, these *subsistence boundaries* are internal boundaries, for example mountain ranges, across which demic diffusion can not take place. We will show later in section 3.2 how these boundaries can give rise to genetic and linguistic anomalies like the Basque.

Since those early modeling attempts, quite a few papers have been published. Most of them focus on obtaining accurate wave speeds i.e. spread rates. The most important one is probably from Fort and Méndez [16] in 1998, where they introduce a time-delayed model by incorporating second-order terms in the reaction-diffusion equation. This allows to model a more realistic form of migration which includes a time delay of one generation i.e. 25 years, between successive migration steps. This time delay leads to overall better results in the spread rate. A different approach is taken by K. Davison *et.al* [17] which focuses on a more realistic environment, as most simulation so far had used homogeneous environments. They argue that diffusion along rivers, especially the Danube and the Rhine, and along coastlines should be faster. In 2004, Kevin Stratford and Graeme Ackland[6] were the first to focus on population interactions and introduced the three populations suggested by Cohen [13]. This project extends Stratfords and Acklands work and uses some of their software.

[6]Both are currently based at the University of Edinburgh

2 Method and Implementation

This section will investigate the model used in this project in more detail. Firstly, the core assumption that the Fisher Equation (1) is a suitable equation for modeling the spread of a population has to be verified. The next step is to explain Cohen's [13] model in more detail and to highlight any modifications and extensions made. Finally, the main steps of how to numerically solve and visualize the model in a computer simulation are explained.

2.1 Finding a solution to the Fisher Equation

In 1937 Fisher [1] introduced an equation, from here on referred to as the Fisher Equation, which describes the spread of advantageous genes in a population. It has been used in many different scenarios and was modified accordingly since then. The for this project relevant form of the Fisher Equation is:

$$\frac{\partial n}{\partial t} = D\nabla^2 n + \frac{1}{\tau} n(1-n) \tag{1}$$

Where n is the population fraction defined as $n = \frac{N(x,y)}{N_s(x,y)}$, $N(x,y)$ being the current population and $N_s(x,y)$ is the saturation population i.e. the maximum population supported at this location. $\frac{1}{\tau}$ is the inital growth rate, which takes population dependent parameters into account and D is the diffusion constant. The first term on the right hand side of Equation (1) is called the *diffusive term* which represents the spread of the population due to the random migration of individuals. The second term is the *logistic growth term* which describes the local growth rate of the population towards a saturation population.

The equation can be reduced to a set of two coupled first order differential equations and solved via a phase space analysis. For a full derivation see section A.1 in the appendix. The calculations show that there exists a positive traveling wave solution (see *Figure 4*) to the Fisher Equation (1) with a wave speed of:

$$\frac{dx}{dt} \geq 2\sqrt{\frac{D}{\tau}} \tag{2}$$

2.2 Cohen's model

For the use in Cohen's model the Fisher Equation is rewritten as:

$$\frac{\partial N}{\partial t} = D\nabla^2 N + \frac{1}{\tau} N\left(1 - \frac{N}{N_s}\right) \tag{3}$$

Where $N(x,y)$ is the population density. Additionally $N_s(x,y)$ is thought to be dependent on land fertility i.e. spatial dependent, which leads to a slightly unfamiliar looking equation.

$$\frac{\partial n}{\partial t} = \frac{D}{N_s}\nabla \cdot (N_s \nabla n) + \frac{1}{\tau(n)} n(1-n) \tag{4}$$

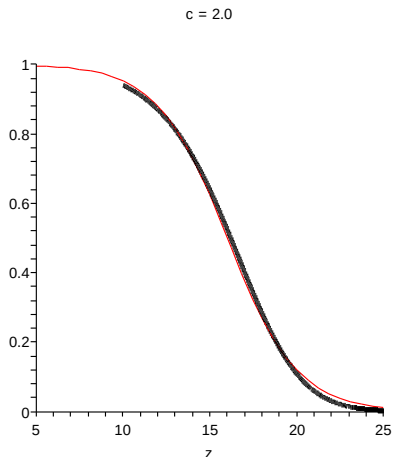

Figure 4: Thick line: the full solution in real space with $Wavespeed = 2$; Thin line: an approximation. In *Figure 10* on page 18 it can be seen that the modeled population wave indeed takes this form.

In the case of a uniform land fertility the first part of the right hand side of Equation (4) becomes $D\nabla^2 n$ which restores the form of Equation (1). The next step is to add a parameter $\sigma(x, y)$, which introduces spatial heterogeneity by assigning each (x, y) position on the model a value which can be thought of as the fertility of the land. We now explore how Cohen's fertility parameter relates to τ and N_s.

Cohen introduces three population-describing parameters.

- The food production per person

$$f = \frac{F_0}{N_0 + N} \tag{5}$$

  where F_0 is the limiting food production capacity per unit area. $N_0^{-1} = A$ is the area exploited per person in the low population limit $N \to 0$. A is assumed to be technology-dependent and therefore culture-dependent.

- The birth rate per person

$$b = \frac{b_0 f}{f_0 + f} \tag{6}$$

  where b_0 is the limiting birth rate and f_0 is the fundamental limit for successful reproduction. Both b_0 and f_0 are assumed to be culture-dependent.

- The death rate per person

$$d = \frac{d_0(f + f_0)}{f} \tag{7}$$

  d_0 is assumed to be a constant biological mortality which is the limiting value if the food production f is high. If the food production drops to zero $f \to 0$, then the death rate goes to infinity.

In the absence of migration, the population change is balanced by the birth and death rate per person and can be written as

$$\frac{\partial N}{\partial t} = (b - d)N \tag{8}$$

Cohen's next step is to assume that the saturation birth rate is culture dependent. The only culturally dependent term so far has been the parameter A. Cohen introduces another culture-dependent parameter $s = F_0 A / f_0$ which can be thought of as the potential of a given location to support a population. By combining Equations (5) and (6), the birth rate can be rewritten as:

$$b = \frac{b_0 s N_0}{N_0(1 + s) + N} \tag{9}$$

This can be simplified further by introducing

$$N_1 = N_0(1 + s) \quad \text{and} \quad b_1 = \frac{b_0 s}{1 + s} \tag{10}$$

to obtain

$$b = \frac{b_1 N_1}{N_1 + N} \tag{11}$$

A similar process is applied to the death rate. By using the definition for s and combining Equations (5) and (7), the death rate becomes population density-dependent:

$$d = \frac{d_1(N_1 + N)}{N_1} \quad \text{and} \quad d_1 = \frac{d_0(1 + s)}{s} \tag{12}$$

Combining the modified equations for the birth and death rates results in a new form for the population change Equation (8):

$$\frac{\partial N}{\partial t} = N \left(\frac{b_1 N_1}{N_1 + N} - \frac{d_1(N_1 + N}{N_1} \right) \tag{13}$$

However, Cohen points out that F_0 and A are not independent. As the food production F_0 increases, s will saturate at a maximum value s_m which relates to the maximal usable amount of food for a society i.e. a further increase in F_0 will not benefit the population. This limiting case can be mathematically expressed as

$$s = F_0 A / f_0 \quad \text{and} \quad A \to s_m f_0 / F_0 \quad \text{as} \quad F_0 \to \infty \tag{14}$$

The other extreme is when food production approaches zero as $F_0 \to 0$. In this case, A can be increased to compensate, but only to a limited value A_M, which is technology-dependent. This finally allows the definition of land fertility:

$$\sigma = F_0 A_M / f_0 \quad \text{where} \quad s \to \sigma \quad \text{as} \quad F_0 \to 0 \tag{15}$$

which introduces spatial heterogeneity to the land exploited by a culture. Interpolating between these two limiting cases allows Cohen to write s and A in terms of a_m and s_m:

$$s = \frac{s_m \sigma}{s_m + \sigma} \quad \text{and} \quad A = N_0^{-1} = \frac{s_m A_M}{s_m + \sigma} \tag{16}$$

The whole model is now defined by only **four parameters** b_0,d_0,s_m and A_M. All of those parameters are culture and technology dependent. This is the basis for a multi-population model. For a population to grow at a particular location, the ratio of the actual birth and death rates, defined as

$$r = \sqrt{\frac{b_1}{d_1}} = r_0 \frac{s}{s+1} \quad \text{where} \quad r_0 = \sqrt{\frac{b_0}{d_0}} \tag{17}$$

has to be greater than one. This can be related to a critical land fertility

$$\sigma_c = \frac{s_m}{s_m(r_0 - 1) - 1} \tag{18}$$

below which the land is not fertile enough to sustain a population i.e. the saturation population Equation (19) vanishes.

$$N_s = A_M^{-1} \left(\sigma \left(r_o - 1 - \frac{1}{s_m} \right) - 1 \right) \tag{19}$$

The logistic growth Equation (13) is then expressed in terms of the fraction of the saturation population $n = N/N_s$:

$$\frac{\partial n}{\partial t} = \frac{1}{\tau} \left(\frac{n_1 + n}{n_0 + n} \right) n(1 - n) \tag{20}$$

where

$$\tau = \frac{d_1}{n_0} \quad n_0 = \frac{1}{r-1} \quad \text{and} \quad n_1 = \frac{r+1}{r-1} \tag{21}$$

In summary, the Fisher Equation (1), incorporating the final version of the logistic growth Equation (20), becomes:

$$\frac{\partial n}{\partial t} = \frac{D}{N_s} \nabla \cdot (N_s \nabla n) + \frac{1}{\tau} \left(\frac{n_1 + n}{n_0 + n} \right) n(1 - n) \tag{22}$$

2.3 Extension to three populations and modifications

We now extend the model by introducing three different populations. Neolithic farmers (n_{NF}), indigenous hunter-gatherers (n_{HG}) and converts (n_X) which are hunter-gatherers who have learned to farm. Since all three cultures could live on one spatial location, the equation for food production has to be changed such that for a population N^i

$$F^i = \frac{F_0^i N^i}{N_0^i + N^t} \tag{23}$$

where $N^t = N_{NF} + N_{HG} + N_X$ is the total population per unit area. Would all involved populations have the same population parameters, for example three farming populations

competing for food in the same region, then their logistic growth term could be expressed as:

$$\frac{\partial N^i}{\partial t} = \frac{1}{\tau^i(N^t)} N^i \left(1 - N^t\right) \tag{24}$$

However since the hunter-gatherers have different population saturation values and different food production rates a more complicated logistic growth equation has to be used and Equation (24) becomes:

$$\frac{\partial N^i}{\partial t} = \frac{1}{\tau^i(N^t)} N^i \left(1 - \frac{N^t}{N_1^i(r^i - 1)}\right) \tag{25}$$

The initial growth rate $1/\tau^i$ is now no longer only dependent on the population parameter b_0, d_0, s_m and A_M but also on the total population N_t. Competition for food resource is introduced and the logistic growth equation for each population can be written as

$$\begin{aligned} \frac{\partial n_{NF}}{\partial t} &= \frac{1}{\tau_{NF}(n^t)} n_{NF}(1 - n_{NF} - n_{NF-HG} - n_{NF-X}) \\ \frac{\partial n_{HG}}{\partial t} &= \frac{1}{\tau_{HG}(n^t)} n_{HG}(1 - n_{HG} - n_{HG-NF} - n_{HG-X}) \\ \frac{\partial n_X}{\partial t} &= \frac{1}{\tau_X(n^t)} n_X(1 - n_X - n_{X-NF} - n_{X-HG}) \end{aligned} \tag{26}$$

The competition for food is accounted for in the cross population terms, which can be generally written as $n_{i-j} = n_j N_{sj}/N_{si}$, where i and j are indices for different populations. Additionally to food competition we introduce technology diffusion in the sense that hunter-gatherers can learn how to farm and become so called converts. We use a simple equation for this conversion factor defining the fraction of hunter-gatherers who become converts per time step as:

$$\Delta n_{HGtoX} = \gamma n_{HG}(n_{NF} + n_X) \tag{27}$$

Where γ is a conversion constant. The equation expresses that the hunter gatherers can learn from either converts or Neolithic farmers. We also introduce competition between the converts and the Neolithic farmers, such that we only allow one population type at any particular location so that there is no population coexistence over time. This can be justified by arguing that there could either be conflicts between the different groups, or in terms of genetics, that the smaller population gets swallowed by the dominant gene pool of the larger population. The hunter-gatherers are not included as their much smaller populations can not compete with neither Neolithic farmers nor converts. A simple formula for this desired behavior is to define the fraction of people changing from the smaller to the larger population by:

$$\Delta n_{NFtoX} = \lambda n_{NF} n_X(n_{NF} - n_X) \tag{28}$$

Where λ is a conversion factor. If $n_X > n_{NF}$ then Δn_{NFtoX} is negative and n_{NF} decreases while n_X increases. One could argue that there is a special case which allows coexistence when $n_X = n_{NF}$, but since this is a unstable equilibrium point we can ignore the special

case. The implementation of those two interactions into Equation (26) gives then the final set of coupled logistic population equations:

$$\begin{aligned}
\frac{\partial n_{NF}}{\partial t} &= \frac{1}{\tau_{NF}(n^t)} n_{NF}(1 - n_{NF} - n_{NF-HG} - n_{NF-X}) + \Delta n_{NFtoX} \\
\frac{\partial n_{HG}}{\partial t} &= \frac{1}{\tau_{HG}(n^t)} n_{HG}(1 - n_{HG} - n_{HG-NF} - n_{HG-X}) - \Delta n_{HGtoX} \\
\frac{\partial n_X}{\partial t} &= \frac{1}{\tau_X(n^t)} n_X(1 - n_X - n_{X-NF} - n_{X-HG}) + \Delta n_{HGtoX} + \Delta n_{NFtoX}
\end{aligned} \tag{29}$$

The diffusion part of the Fisher equation (30)

$$\frac{\partial n}{\partial t} = \frac{D}{N_s} \nabla \cdot (N_s \nabla n) \tag{30}$$

was not modified with the exception of the diffusion constant D. Initial test have shown that the simulated population wave front expanded with constant speed regardless of the altitude. After a discussion with Graeme Ackland we agreed to make the diffusion constant D altitude dependent, as it seemed realistic that the migration should be slowed down by mountain ranges. The simple form used to achieve this is the creation of a linear dependence on altitude. For example, if the diffusion should be slowed down by 99% at the highest point on the grid-map, then

$$D_{modified}(x, y) = D - \frac{0.99 \times D \times altitude(x, y)}{\text{max. altitude on grid}} \tag{31}$$

2.4 Software Implementation

In the previous sections we have developed a model and proven that the underlying Fisher equation is a suitable basis formula for our model. This section will highlight the main steps of implementing our model into a computer simulation.

The first step is to acquire suitable data to build a realistic, inhomogeneous land model. The raw data for this land model comes form the National Geophysical Data Center (NGDC) of the United States. The NGDC offers a web service[7] which allows to customize a data grid for which boundaries can be specified as longitude and latitude values. The grid is discretized in a maximum resolution of 2 minutes of arc and contains the average altitude value of each grid field. This data grid is then changed to a lower resolution of 6 minutes of arc, as the 2 minute resolution would result in too large files, and converted to a two dimensional array within the computer model. The altitude data can then be modified to allow an adjustment of the sea level to create a map of Europe as it may have looked like 10,000 years ago. See *Figure 5.* Note that some of the "lakes" that appear on the picture are actually dry areas which are below sea level. The software can not compensate for this errors, but they don't have major effects on the simulation outcome.

[7] http://www.ngdc.noaa.gov/mgg/gdas/gd_designagrid.html

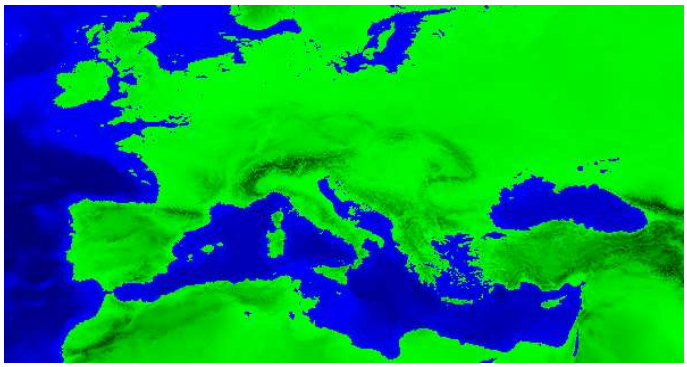

Figure 5: Europe land model: Bright green = low altitude; dark = high altitude;

The next step is to develop a temperature model. Temperature data can be obtained from internet resources but unfortunately not in a high enough resolution to fit the resolution of the land model. A simple temperature model was developed in which temperature is a function of longitude, latitude and altitude. The parameters were first adjusted in such a way as to obtain a similar picture to that of the real data, but then further cooled down to simulate the retreating glaciers. See *Figure 6*.

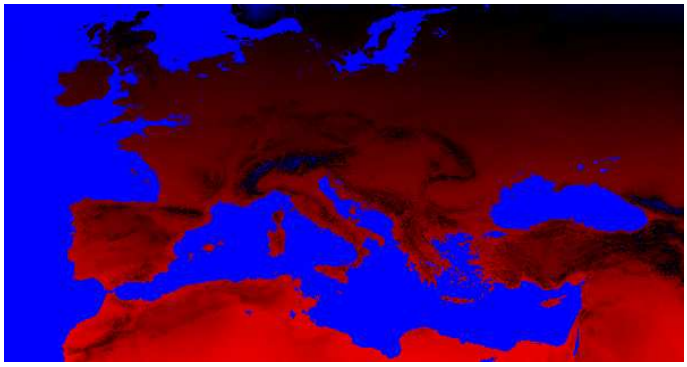

Figure 6: Calculated temperature map of Europe, bright red = hot and black/blue = cold.

An important point to keep in mind is the fact that the given altitude data is from the surface of Earth which is a sphere, but two dimensional software arrays are inherently flat i.e. a plane. So a data conversion is necessary to map the spherical data onto a plane. For the Norther Hemisphere the shape of a grid-point $P(x, y)$ is illustrated in *Figure 7*. If the Earth is assumed to be a perfect sphere, then the distance between Latitude-lines dy will be constant. So each grid-point will have the same "height" dy. However, the Longitude-lines converge at the pole, which implies a smaller "width" dx of grid-points further north. Additionally it is necessary to distinguish between the upper and lower width, dx_{upper} and dx_{lower} respectively. These values can be estimated by calculating the circumference L of Earth around the Equator (at Latitude angle $\theta = 0$) where $L = 2\pi * R_{Earth}$. Dividing L by 360° gives the length of one degree $dx_0 = L/360$

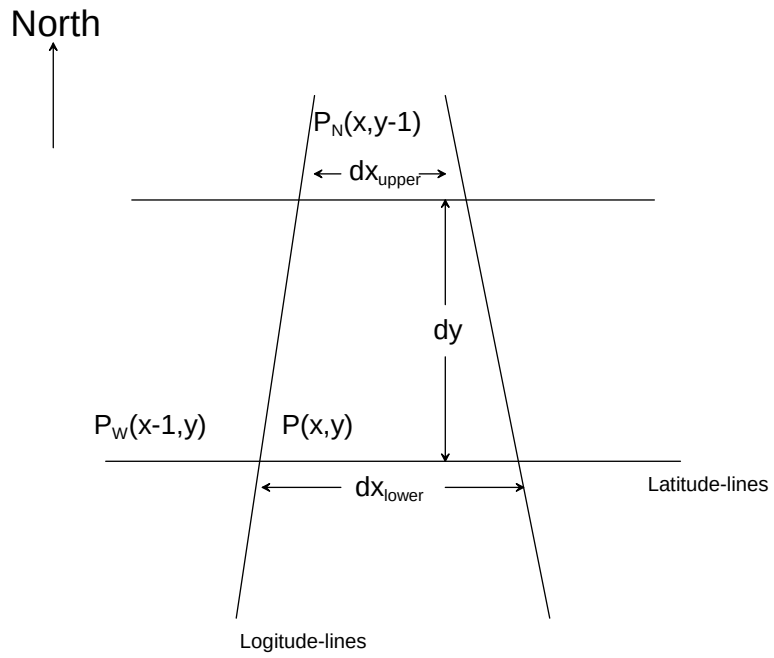

Figure 7: Mapping of spherical surface onto a flat plane

at the Equator. The length of one degree at any angle θ between the equator and the pole i.e. $0 \leq \theta \leq 90$, is then just $dx_\theta = dx_0 * \cos\theta$. So although the way the simulation displays the maps, in a one pixel per grid-point fashion, implies a homogenous spaced grid, the underlying calculations were carried out on the realistic grid displayed in *Figure 7*.

The final step is to solve the equations established in section 2.2. This is done via a discretisation based on an Euler forward step.

$$n^{t+1} = n^t + \Delta t(\text{Diffusive-part}(n^t) + \text{Logistic-part}(n^t)) \tag{32}$$

The implementation of the logistic-part of the equation is straight forward, as the logistic equations (29) can be solved easily. The diffusive-part requires the definition of fluxes across grid-point boundaries. This is done in a "four nearest neighbors" approach, to avoid the problem of defining fluxes across a zero-width boundary for the diagonal neighbors. For a detailed description of how the fluxes are calculated please see section A.2 in the Appendix.

3 Results & Discussion

This section will explore in detail the simulation results obtained in the four different scenarios. The main focus will be on Europe as it is the region where most archaeological evidence is available. The India and South Africa scenarios are experiments which further expand the model, but are not as detailed as the European scenario. The screen shots used in this section are only a limited visualization of the dynamic spread of the Neolithic farmers. Fully animated movies of each scenario are available on the CD-Rom attached to this report.

3.1 The Test Area

The test area was developed for several reasons: To create a feeling for the model parameter, to display the advancing wave front and to measure the wave speed. The used land data is an artificial map with a Gaussian shaped mountain range which is symbolized by the dark area in the middle of the map. The same spatial resolution (six minutes of arc) as for the other scenarios, is used. This is done so that suitable parameters which give the correct wave speed in the test area can be directly ported to the other scenarios. The main population parameters used (see Table 1) are based on Kevin Stratfords values and are similar for the three different populations, with the exception that the birth rate of the hunter-gatherers is only 40% of the birth rate of the Neolithic farmers and that their minimum living area A_M is 50 times larger.

Parameter:	**Neolithic Farmer:**	**Hunter Gatherer:**	**Converts:**
Maximum Birthrate b_0	0.06	0.4*0.06	0.06
Maximum Deathrate d_0	0.02	0.02	0.02
Minimum Area A_M	1	50	1
Maximum Food-production s_m	50	50	50

Table 1: Basic population parameters used in all four scenarios.

Ammerman and Cavalli-Sforza [12] argue that a four year birth interval would be suitable for the hunter-gatherer lifestyle, where it is convenient for a women to carry only one small child at a time. A high birth interval will assure that a child is independent enough to keep up with its parents' pace, before the next is born. In the case of a farming culture, children can be more useful and Ammerman and Cavalli-Sforza estimate a birth interval of about two years. The multiplication of A_M by 50 represents the nomadic lifestyle of the hunter and gatherers.
The user interface for the test area can be seen in *Figure 8*. The left column shows the Neolithic farmers where the top display is the normal view with the farmers superimposed on the land. Farmers are shown in shades of red and the land in shades of green. The initial farming population is displayed as a single orange point. The graph underneath shows the population fraction $n = N/N_s$ along a single line in the x-direction of the map.

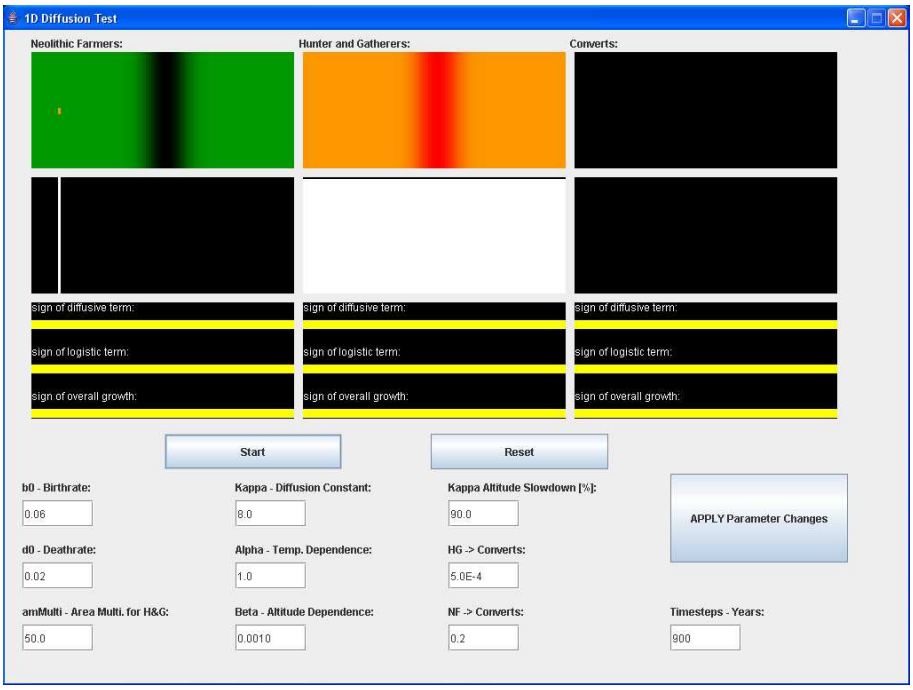

Figure 8: The user interface of the Test Area.

The white spike indicates the starting position of the farmers where $n = 0.99$. The final display in the column visualizes the signs of the diffusive term (yellow = zero, red = positive and blue=negative), the logistic term and the overall population growth along the same line in the x-direction as in the display above. It has mainly been implemented for debug reasons and will not be discussed further.

The middle column shows the already pre-distributed Mesolithic hunter-gatherers and the right column the convert population. Note that there is no land background in the top display of the convert column due to better contrast because the halo formed by converts can be very weak. In *Figure 9* the diffusion process has just started. Note how the initial

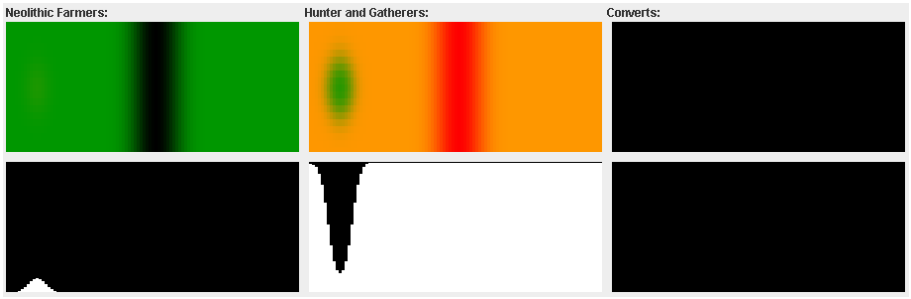

Figure 9: Start of diffusion

spike (or delta function) of the farming population has spread out to a small Gaussian shape. In the center column, the hunter-gatherers get overwhelmed. Note that the spread does not appear to be circular. This is only due to graphical scaling reasons. In *Figure*

10 the farmer population has grown and the diffusion has advanced. The measured wave

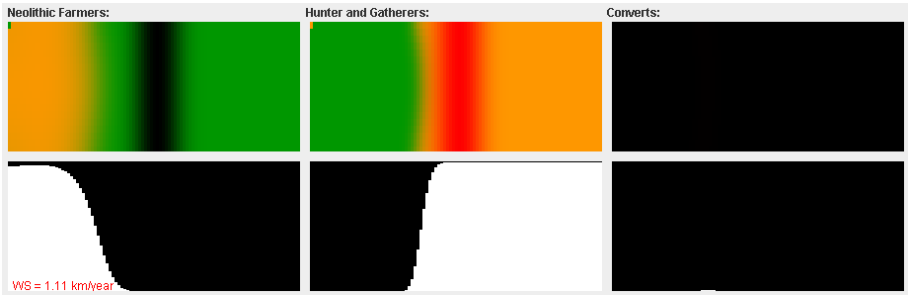

Figure 10: Wavefront formations

speed is approximately 1.1 km per year and the wave front shows the expected form, which was derived in section 2.1. Both are good indications that the used parameters, which to a large extend were taken from Kevin Stratford's simulation, seem to be suitable for the other scenarios.
Figure 11 shows how the altitude-dependent diffusion constant D results in a slowdown of the wave as it reaches the mountain range. The wave form becomes much steeper

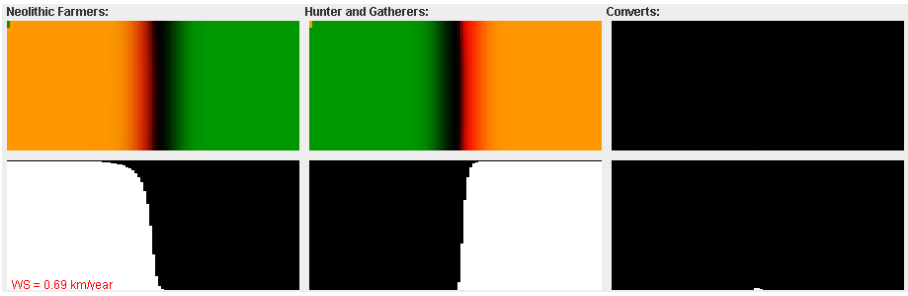

Figure 11: Slowdown at the mountain range

and the wave speed drops significantly. We have argued in section 2 that this is a more realistic behavior than a constant diffusion rate. A constant D would result in a wave front which ignores the presence of the mountain range and continues without a slowdown or deformation. In the third column, a small halo of converts is noticeable. In *Figure 12*, the wave leaves the mountain range behind, it restores its shape and increases its speed again. The halo of converts traveling in front of the farming wave is now more noticeable. The creation of the converts is a direct result of Equation (27), where we introduced the conversion from hunter-gatherers to converts. The converts are treated as an exact copy of the Neolithic farmers, i.e. the share the same population parameters. However, the converts would be overwhelmed by the wave of Neolithic farmers following them, if the competition equation (28) had not been introduced. It favors the larger of either the farmer or the convert population, and since the halo of converts is at the front of the Neolithic farming wave where there are only few farmers, it can grow over time. Eventually the converts can become the dominant population and take on the role of farming technology carriers. What is interesting is the transition point at this change

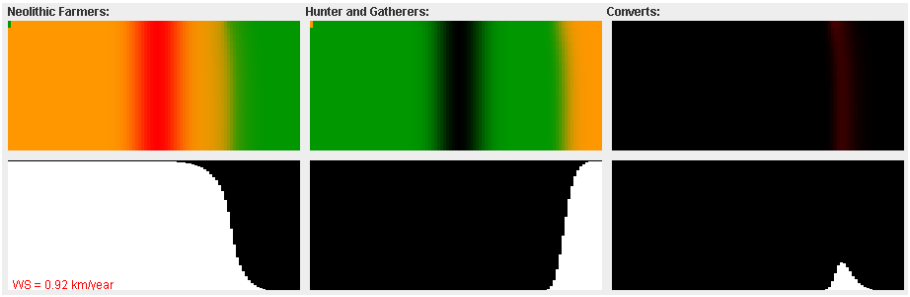

Figure 12: Start of diffusion

occurs, as roles seem to reverse. The converts become dominant and spread farming and the Neolithic farmers become a halo traveling in front of the convert wave, eventually dying out. The described behavior is observable in the screen shots in *Figure 13*.

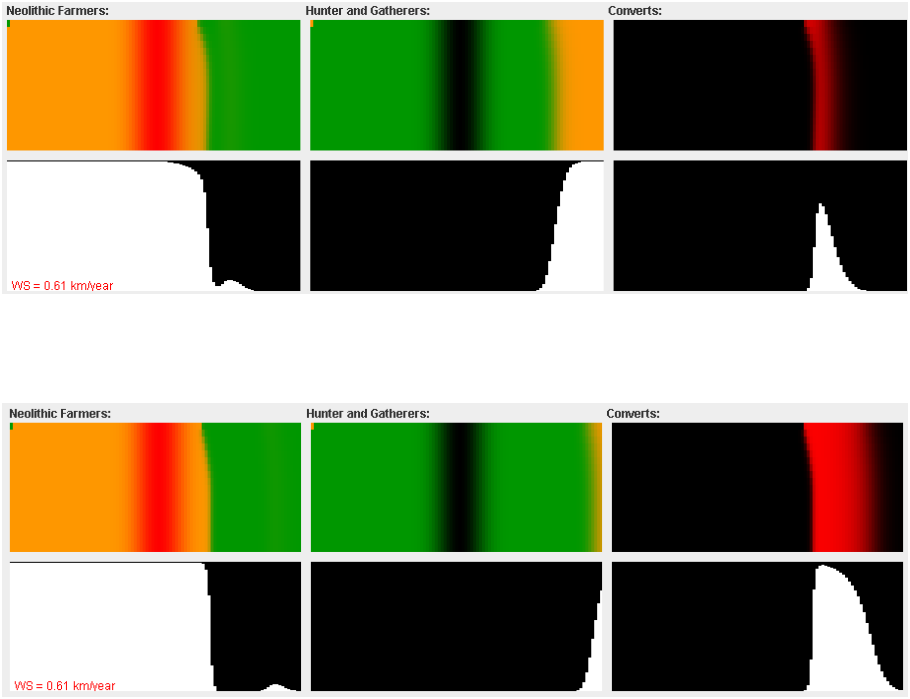

Figure 13: After the transition point (*above*) the converts have become the dominant population(*below*).

3.2 Europe

Europe is the scenario for which most archaeological evidence is available. However, there is still an ongoing debate in the fields of archaeology, linguistics and genetics of how exactly the Neolithic transition happened and how relevant it is for explaining certain characteristics of modern Europe.

As numerous as the different opinions of scholars are the possibilities to influence the outcome of simulations by using different parameters. I am therefore very much aware that people sometimes claim that simulations seem to be parameter-tweaked until they show the desired results, and that such claims seem possible for this simulation. It is therefore important to remember that this report does not claim to have found the exact answer to the question of how the Neolithic transition took place. It merely tries to establish links between possible simulation outcomes and existing theories which could put constraints on the origin of certain aspects of Europe.

In this section we will try to consider certain aspects of the Neolithic transition in Europe by means of following the time-line of a single simulation run. *Figure 14* shows the

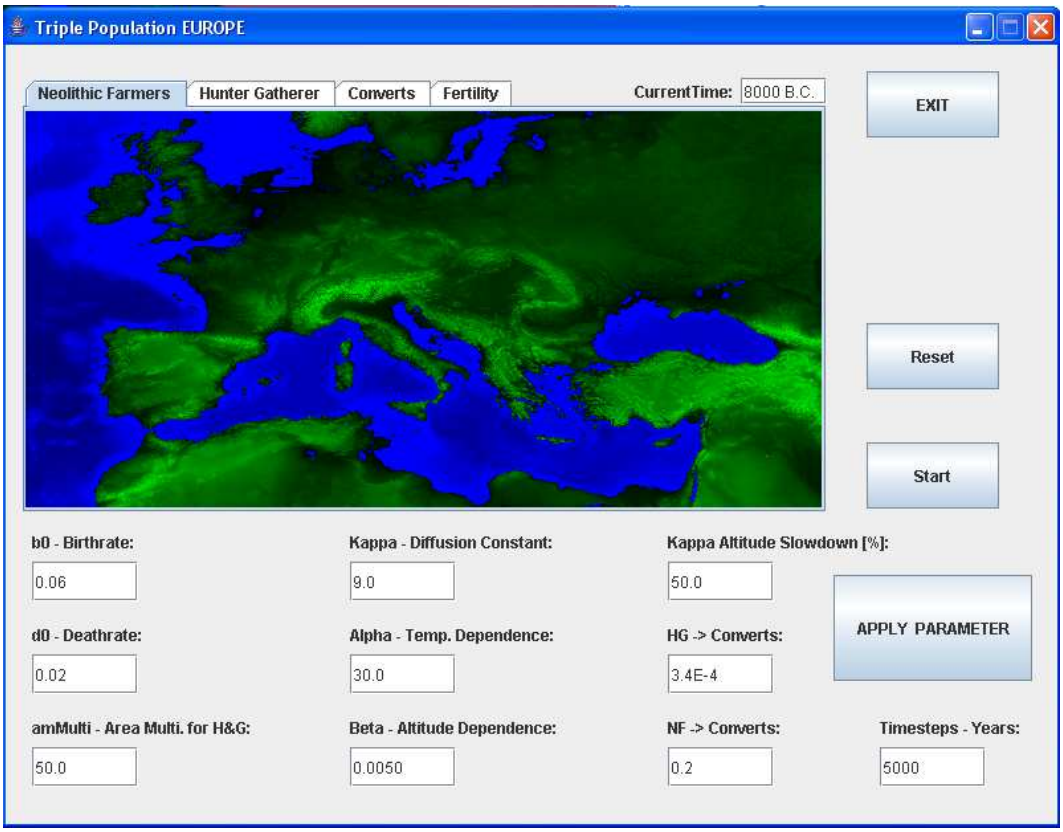

Figure 14: The user interface of the European scenario

user interface of the Europe scenario. The currently tabbed display shows the Neolithic farmer distribution, which is to start with just a single point in the Middle East. The parameters used for the simulation run are the ones shown in the screen shoot in *Figure 14*. *Figure 15* contains screen shots of the hunter-gatherer tab (on the left) which shows the pre-distributed hunter-gatherers in red. The central Alps, parts of Scotland, the Caucasus and the northern regions of Scandinavia and Russia are not occupied because land fertility is too low. The image on the right is the fertility tab. It displays fertile areas in bright green and infertile areas in dark colors. After the start of the simulation, the Neolithic farmers begin to spread out spherically and the hunter-gatherers get displaced, see *Figure 16*. A convenient way to estimate the wave speed is to measure the time

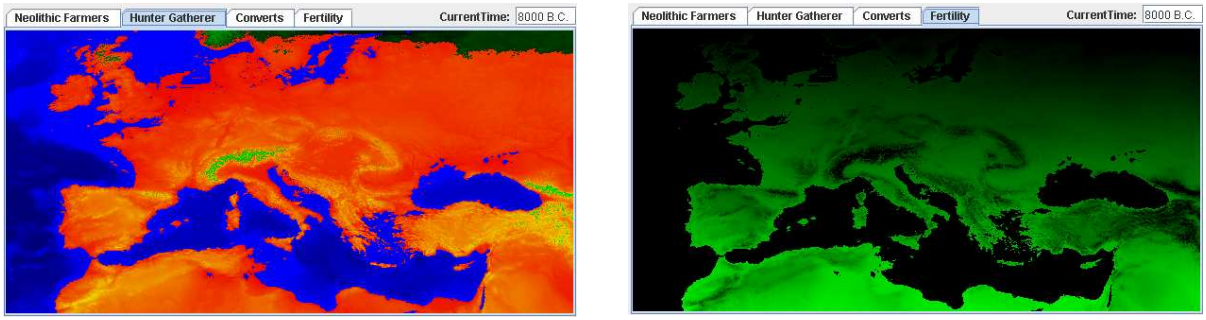

Figure 15: The pre-distributed hunter-gatherers (*left*) and the fertility model (*right*).

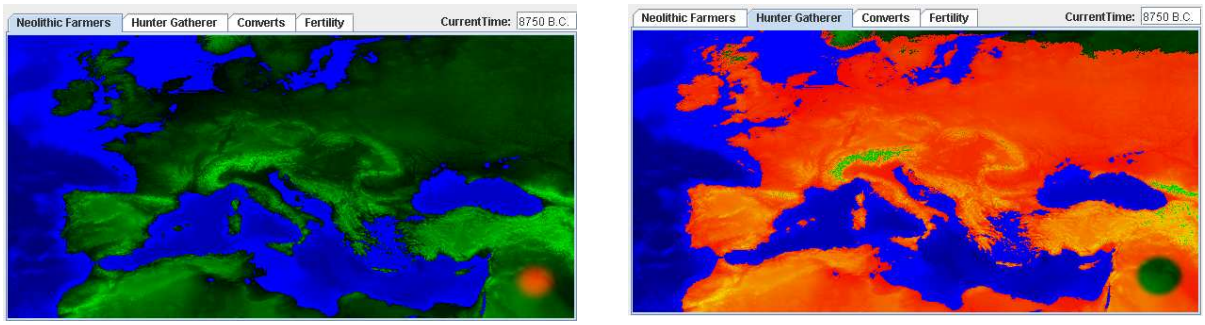

Figure 16: The Neolithic farmers start spreading spherically (*left*) and the hunter-gatherers get displaced (*right*).

it takes from the start of the simulation until the wavefront has reached a prominent point on the map. A well-suited location for such a measurement is the city of Istanbul. Situated on both sides of the Bosphorus, it is easy to estimate its location on the map. A great circle distance calculation between the starting location at (34° North/41° East) and the location of Istanbul (40°58′ North/28°50′ East) gives a distance of about 1400 km. So if the wave speed is about 1.0 km per year, then the wave front should reach the location of Istanbul at about 7600 B.C. *Figure 17* shows that this is indeed the case. Another interesting fact revealed by the same image is that migration takes place along

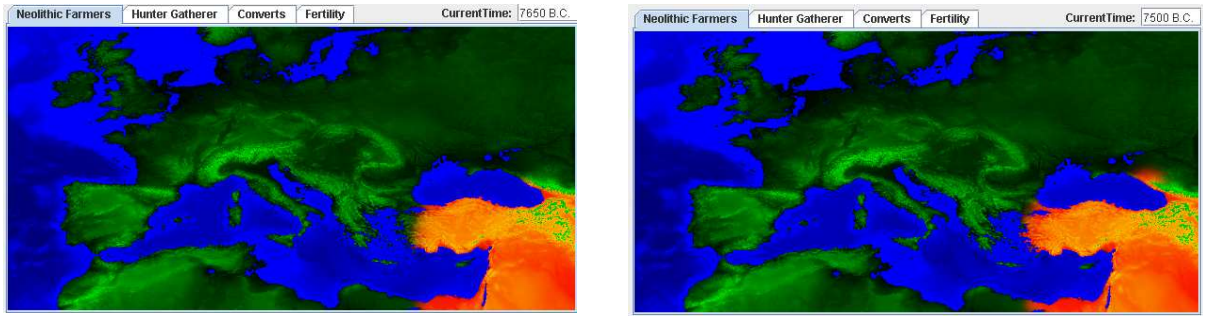

Figure 17: The wavefront reaches the location of modern Istanbul, having traveled about 1.400 km in 1.400 years (*left*) and having passed the bottlenecks of Caucasus and Bosphorus(*right*).

the east coast of the black sea which effectively avoids the obstacle represented by the Caucasus mountain range. This is another point of discussion between scholars as some argue that farming technology was introduced in the areas north of the Caucasus by a

route across the Bosphorus and around the west coast of the Black sea. However, it seems reasonable that migration might have taken place along the west and east coast line like this simulation suggests. A further argument towards this possibility is provided by William Ryan and Walter Pitman from Columbia University who argue in their book [18] that the Black sea was once a fresh-water lake who's surface was more than 100 m lower than it is today. They argue that by 6500 B.C. the rising sea level breached the Bosphorus land bridge and salt water was pouring into the Black sea basin at a very high rate. This event might had be at the core of Noah's Flood described in the Bible. Regardless of this connection, if the breach happened around 6500 B.C. with the first farmers having reached the lake more than a thousand years earlier, it is very likely that they found ideal conditions to farm along the shoreline of the lake and nothing indicates that they did not spread around the lake in both directions.

Having left the bottlenecks of the Caucasus and the Bosphorus behind, the Neolithic farmers spread further north and west. By the time they reached the fertile loess soils of the Danube area, the halo of converts (see Figure 18) which was already observed in the

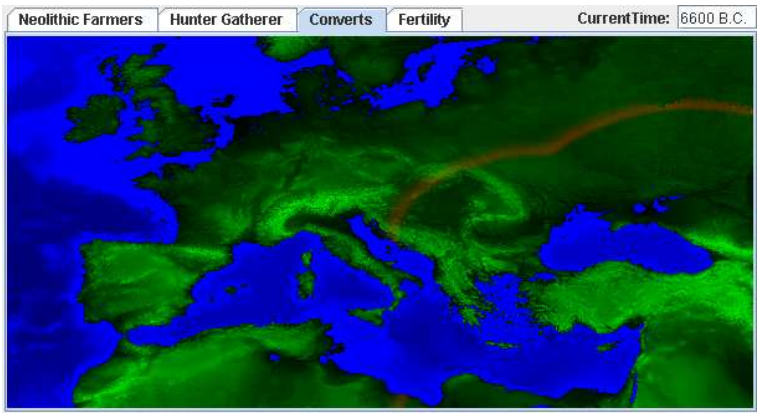

Figure 18: The halo of converts traveling ahead of the Neolithic farmers

test area earlier, has become so large that the converts become the dominant population. From that point onwards the converts act as the technology carrier who brings farming into Europe. Marek Zvelebil [19] [20], an archaeologist from the University of Sheffield, does not believe in the wave of advance model, but thinks that the spread of farming happened in a "leap frog" advance. The "leap frog" model is another theory which is popular with scholars who don't believe in the population explosion necessary to sustain the wave of advance model. They think that small isolated enclaves of farming were formed on the basis of small scale migration. Those small farming enclaves passed the knowledge of farming onto the local hunter-gatherers via cultural interaction and that the so created converts spread farming to the rest of Europe.

Zvelebil reproduces a map (see *Figure 19*) of "colonist" and "indigenous" regions, which shows that Neolithic farmers settled in Turkey, Greece and the Danube area[8], but the rest of Europe is populated by Mesolithic hunter-gatherer descendants who have learned to farm and are effectively converts. If the model used by this project would

[8]A fact that actually contradicts Zvelebil's "Leap Frog" model.

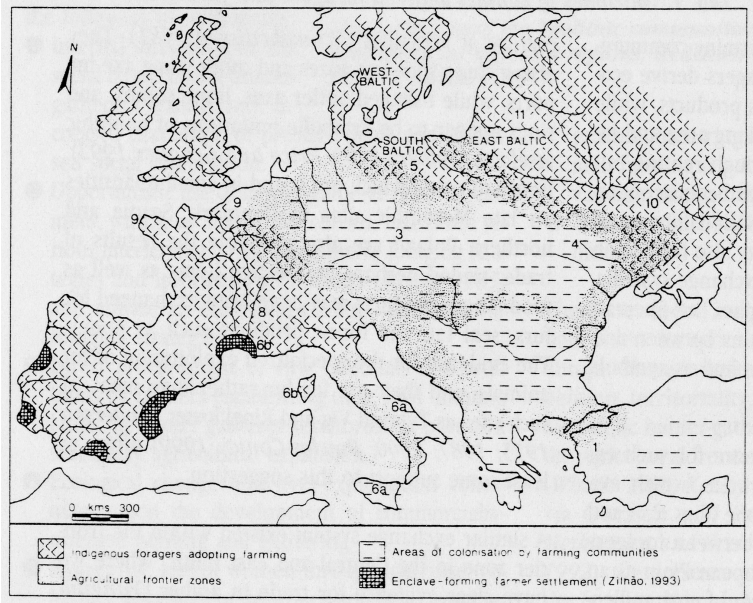

Fig. 1. 'Colonist' and 'indigenous' regions of Europe at the agricultural transition according to one (integrationist) interpretation of the archaeological evidence. Base map after Renfrew (1986) with additional information from Zvelebil and Zvelebil (1988) and Zilhão (1993).

Figure 19: Horizontal lines show settlement of Neolithic farmer, diagonal lines of Mesolithic hunter-gatherer who have learned to farm.

have implemented a higher diffusion rate along rivers, similar to [17], then Zvelebil's map could almost be perfectly reproduced.

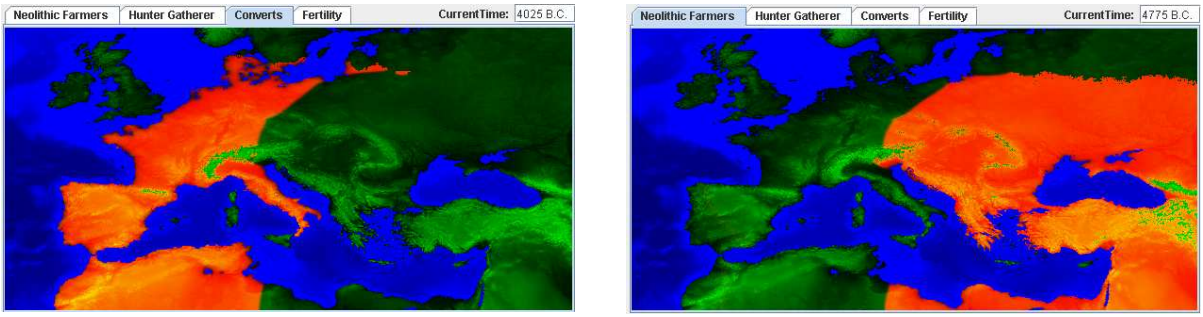

Figure 20: The converts spread farming to the rest of Europe (*left*) and the expansion of the Neolithic farmers halted (*right*).

Farming reaches the far south west of Europe by about 4500 B.C (see *Figure 20*), but it fails to reach the British isles as the land bridge across the Channel vanishes about 6500 B.C., at a time where the farmers have only reached the Danube area. However, there is archaeological evidence that farming did reach Britain by 4000 B.C. which implies that shipping must have been sufficiently developed. Further evidence of sea travel in the early Neolithic is the settlement of Crete [7] by 6.000 B.C. Both highlighted points, fast diffusion along river lines i.e. along the Danube and sea travel, would be valuable additions to the current model.

So is there evidence for the Basque to be descendants of Europe's Mesolithic hunter-gatherer population according to this model? *Figure 21* does not really indicate a large isolated group of hunter-gatherers in the region of today's Basque country. The isolated

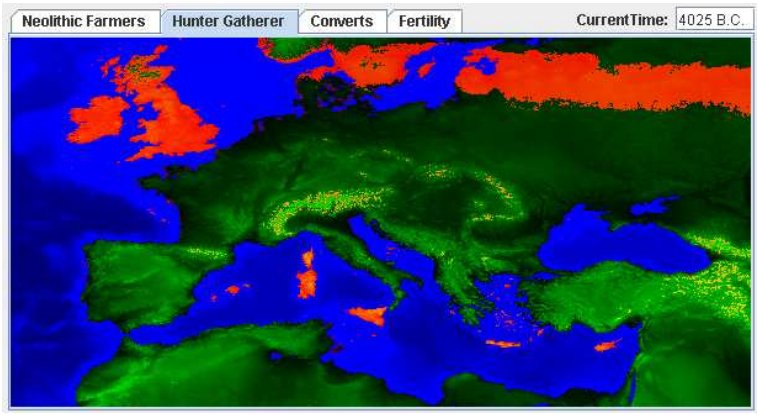

Figure 21: The remaining hunter gatherer populations after the Neolithic transition.

regions in the Pyrenees are too small to be the origin of the Basque. However, if we regard the switch between farmers and converts visible in *Figure 20* also a language border then it might still be possible. If the converts kept their own language, then Basque country would be occupied by a farming population which still speaks the language of the hunter-gatherers. One could further argue that due to later events in European history, the prominent language barrier shown in *Figure 20* was wiped out due to invasions from the east, large people movements and the Roman occupation. All these events would have created a homogenous language background which Europe actually has, with most of its languages being members of the Indo-European language family. Nevertheless, it could have be possible for a remote area such as Basque country to have maintained its language. Further more we can draw the conclusions that shipping must have been sufficiently developed to allow the crossing of the British channel, as the simulation shows that the farmers would not have arrived in time to use the land bridge.

3.3 India

India is a very diverse country. Its fertile land has attracted many different cultures at many different times. What makes India stand out in comparison to Europe, is the fact that cultural differences did not get absorbed or eliminated but remained as isolated sub cultures, thereby creating a large cultural diversity. Within India, there exists a total of four language families: Austric, Dravidan, Indo-European and Sino-Tibetan. Two largest are the Indo-European family in the north-west and the Dravidan family in the south-east. There is considerable scholarly debate on what event brought the Indo-European language family to India. Most academics think that it spread together with the domestication of the horse (around 4000 B.C. at the shores of the Black sea) or the use of iron (around 3000 B.C. in Anatolia) [21]. The application of the wave of advance model to the India case highlights the possibility that the Indo-European language could have arrived with

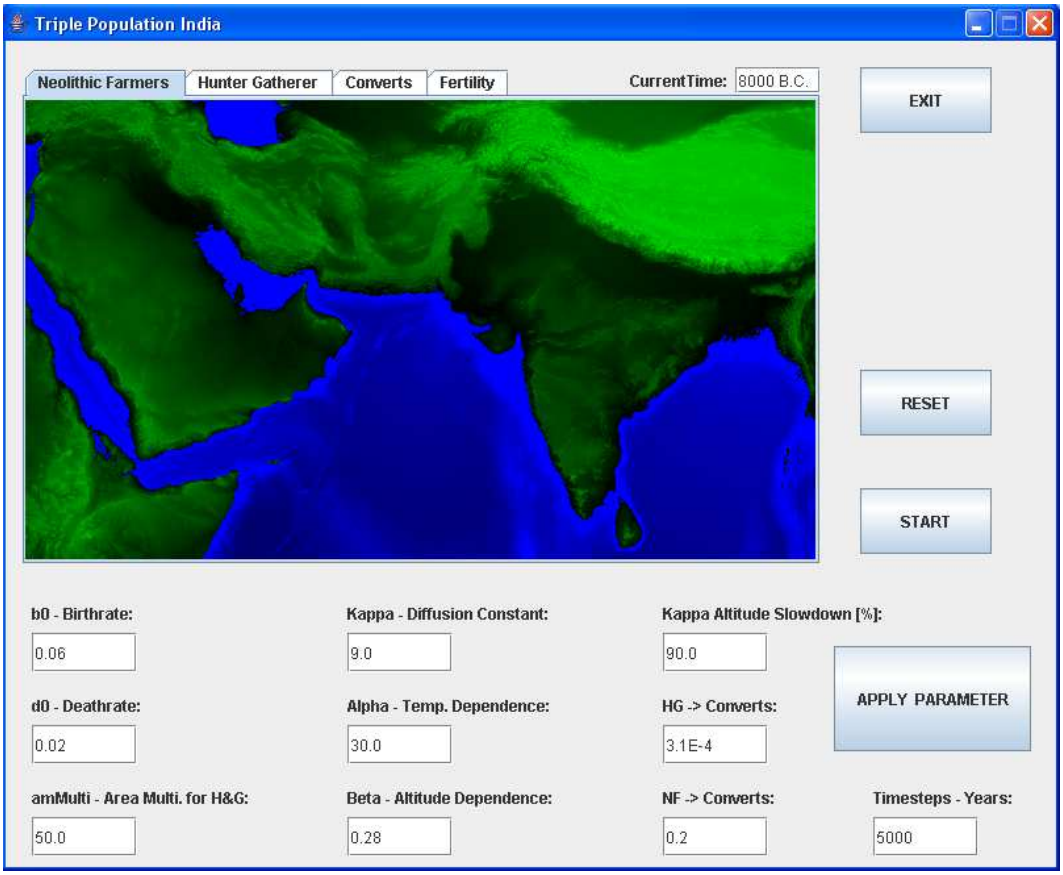

Figure 22: The user interface of the India scenario.

farmers migrating from the Fertile Crescent. The simulation parameters used can be seen in *Figure 22*.

The starting position and date of the Neolithic farmers are the same as in the European scenario in Section 3.2. The farmers spread out spherically from their origin in the Fertile Crescent and follow the coast line of Iran and Afghanistan towards India. A similar

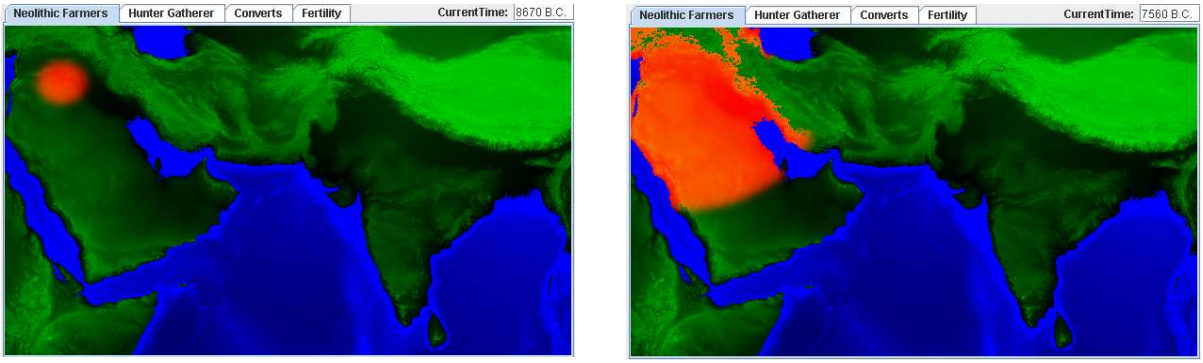

Figure 23: Neolithic farmers start spreading (*left*) and follow the coast of Iran and Afghanistan towards India (*right*).

switch to the one in Europe between Neolithic farmers and converts occurs as the wave

of advance reaches the north-west of the sub continent, see *Figure 24*. The exact location of this transition is of course parameter-depending, but more important than the exact location is the fact that such a switch does occur. It implies the possibility of a language

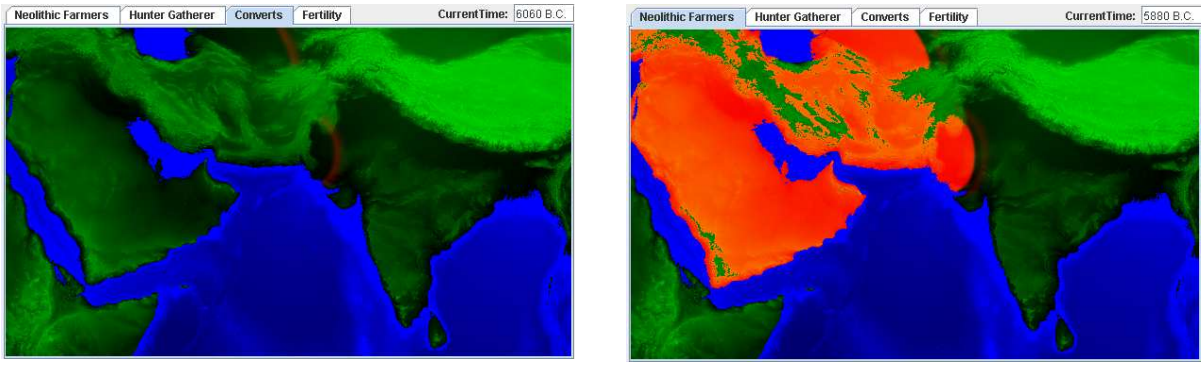

Figure 24: The halo of converts ahead of the Neolithic farmers(*left*) The switch has occurred and the Neolithic farmer form a halo ahead of the converts(*right*).

change if the assumption is made that the Indo-European language was carried to India by the Neolithic farmers. The converts could then spread farming further into the sub continent but keep their own language (possibly Dravidan). Strong evidence for the spread of farmers from the Fertile Crescent to India is given by Cavalli-Sforza in [10] where he compares the results of a genetic analysis of the first principal component for

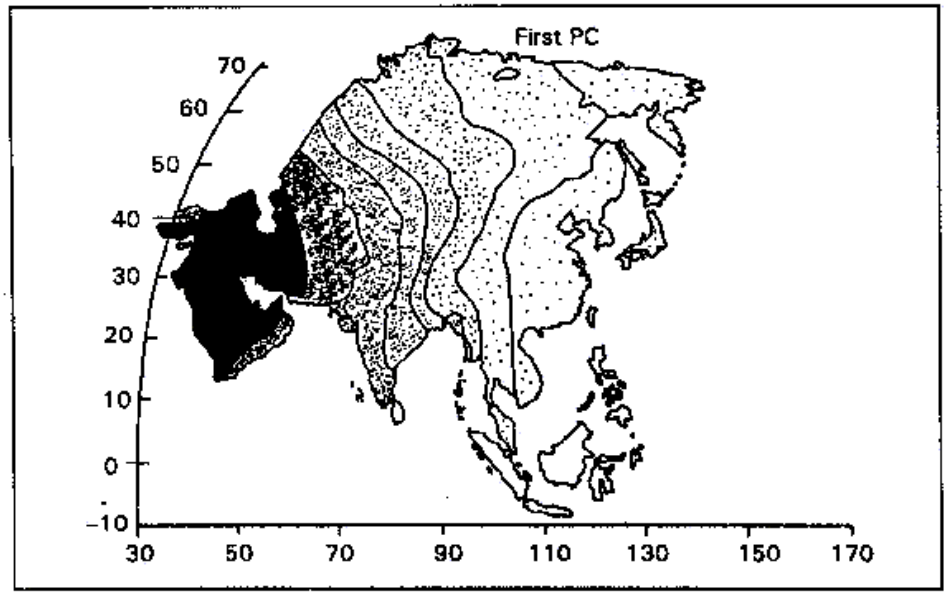

Fig. 6 *Synthetic genetic map of the first principal component for Asia based on 69 genes for 42 populations [Cavalli-Sforza et al., 1994]*

Figure 25: Genetic map of the first principal component for Asia based on 69 genes from 42 populations. Reproduced from Cavalli-Sforza [10].

Asia, based on 69 genes from 42 populations. The map of the first principle component,

shown in *Figure 25*, resembles the simulation outcome. Additionally, by comparing the regions which speak Dravidan today with the final simulation outcome in *Figure 26*, it seems possible that the Neolithic transition might be partly responsible for the language

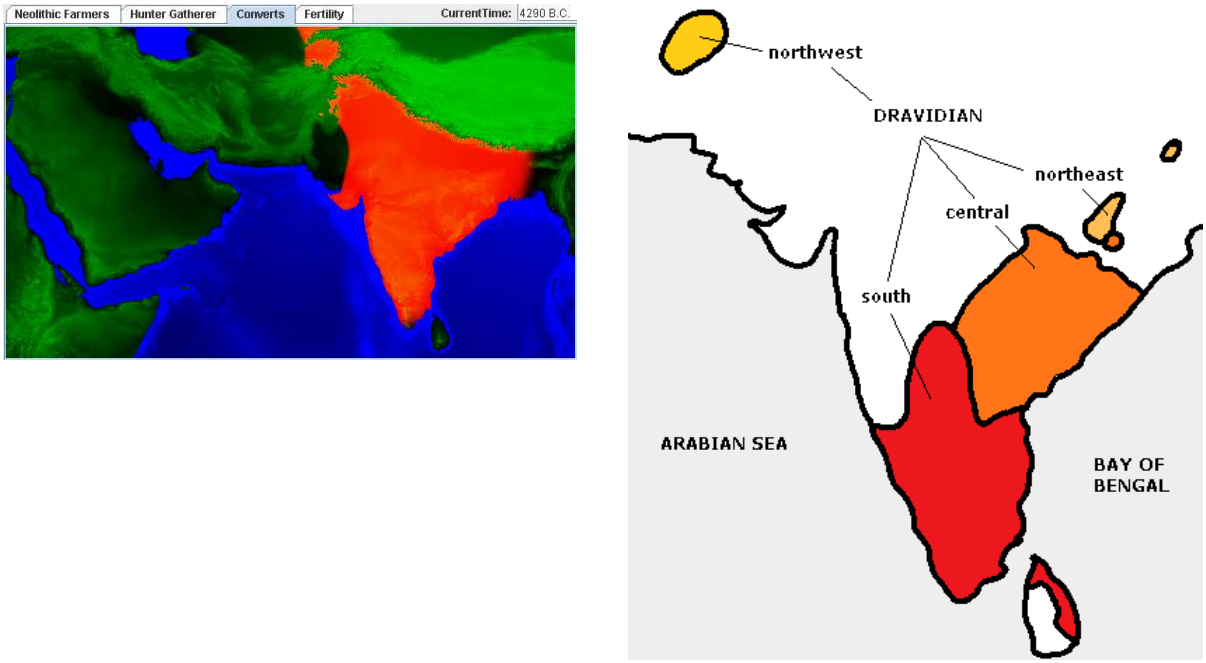

Figure 26: The convert population at the end of the simulation (*left*) The regions of India in which Dravidan is spoken today.(*right*).

regions in India. Madhav Gadgil [21] argues for a different scenario. He thinks that the Neolithic farmers spoke Dravidan and that the Indo-European language came later to India with either the Horse or Iron, and that a second farming population coming from the east is responsible for the language barrier.

However, it seems odd that the same people who carried the Indo-European language to Europe should speak a different language on their journey east. Based on this arguments we can conclude that the simulation outcome can indeed be a possible scenario to explain the existence of a language barrier and the presence of farming, without referring to a second farming population coming to India from the east.

3.4 South Africa

When the first European settlers set foot on South Africa's soil in 1652 (employees of the Dutch East Indian Company), farming had not yet reached the south tip of Africa. The reason for this was that the crops which were used by the indigenous African farmers were not suitable for the climate of South Africa. These were crops which originated in the tropics and sub-tropics around the Congo river. When the European settlers, who had brought with them wheat and barley, started to expand northwards and came in contact with the African farmers, the latter adopted wheat and barley for themselves. This allowed them to expand further south.

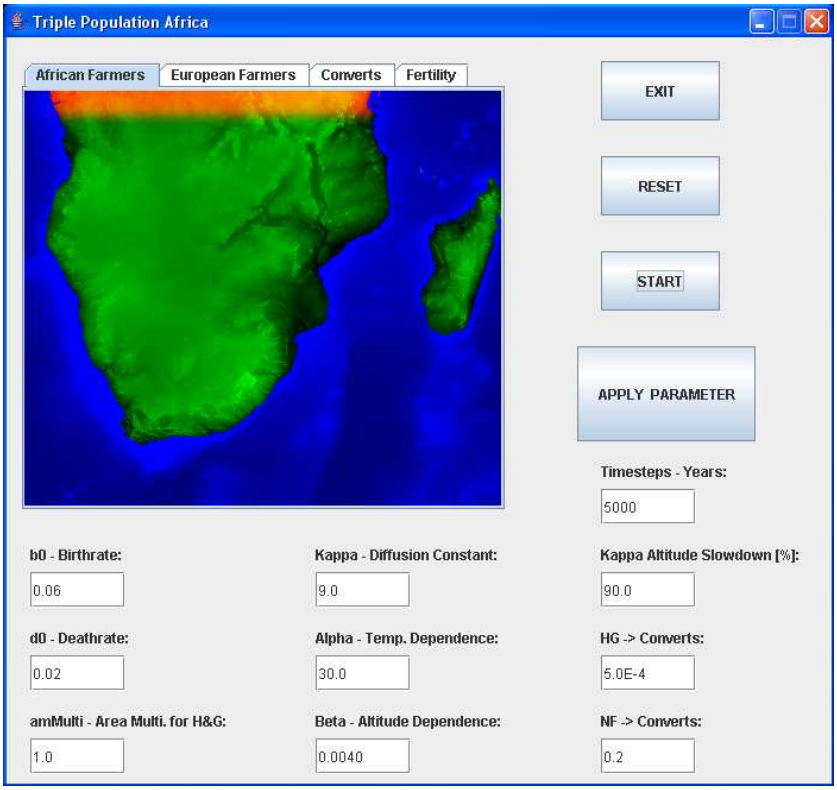

Figure 27: The user interface of the South African scenario with the initial African farmers in the north.

Although this is a scenario for which this model is not really suited because it does not allow co-existence of farming populations, we nevertheless applied it to see if it would be possible to trigger the event where African farmers adopt new crops and start spreading south. For this simple test realistic population starting points are neglected and the

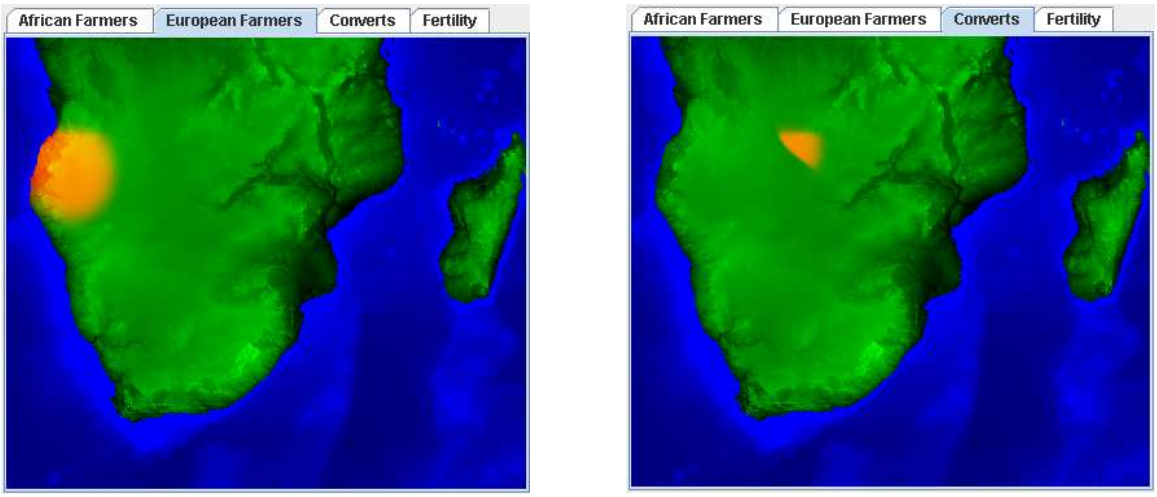

Figure 28: The European farmers spreading out(*left*) and the first formation of converts spreading south.(*right*).

scenario map is extended to encompass the area south of the tropics. The diffusion of African farmers to the south is restricted, but a population of converts (African farmers who have come in contact with the European farmers and adopted their crops), can move south. *Figure 28* illustrates the formation of converts as soon as the European farmers

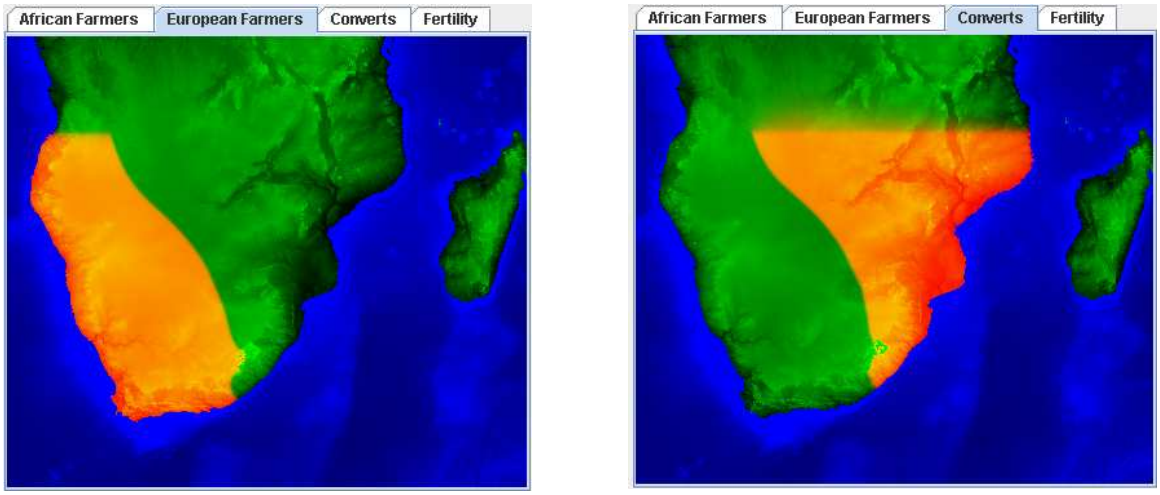

Figure 29: Both, European farmer (*left*) and the converts (*right*) have spread all the way south.

make contact with the African farmers. From that point onwards the converts start spreading out and compete successfully with the European farmers. Both take control of about half the land mass available as seen in *Figure 29*.

We can conclude that the model served to simulate the trigger event, the passing of new crops to African farmers. In order to model the actual historical events more realistically, it would be necessary to allow for populations to co-exist peacefully. In addition it would be necessary to research more accurately the starting points for the populations. Unfortunately there was not enough time left to do this, but this little side scenario has shown that it would be possible to apply the model to a range of other scenarios than Europe, for which it was originally developed.

4 Conclusion

Unlike physics, archaeology and linguistics are not always exact sciences, especially if an attempt is made to link events which occurred 10,000 years ago to the present. I therefore have to acknowledge that the obtained simulation outcomes and the conclusions drawn in the previous section are by no means exact results.

However, I think that this project has shown that a model based on physical principles i.e. the diffusion equation, can be successfully applied to scientific areas outside classical physics and is able to reproduce archaeological evidence. It can help to investigate different theories and to visualize difficult processes. The visualization of complex systems can be of great help to gain a better understanding of how systems work.

One of the main efforts of this project was the development a software platform and a model which could be easily expanded. From here, one could add more detailed population interactions, apply the model to different scenarios and gain a better understanding due to the detailed visualizations this software provides.

5 Acknowledgments

I would like to thank

- Kevin Stratford for allowing me to build my project on his existing Javaman model.
- Graeme Ackland for helpful discussions and guidance.
- Marek Zvelebil for sending me his publications and having time for an undergraduate.
- Andrew Jones for help with jpeg's.

References

[1] **Fisher, R.A.** *The wave of advance of advantageous genes*; Annals of Eugenices, V.7: p355-369 (1937)

[2] **White, T.D. et.al.** *Pleistocene Homo Sapiens from middle Awash, Ethiopia*; Nature 423: p742-747 (2003)

[3] **Cavalli-Sforza, Luigi Luca and Francesco** *The Great Human Diasporas - The History of Diversity and Evolution*; ISBN 0-201-44231-0, 1993

[4] **Oppenheimer, Stephen** *The Real Eve: Modern Man's Journey Out of Africa*; ISBN 0-786-71192-2, 2003

[5] **Harlan, J.R. ,*et.al.*** *The Origins of Agriculture and Crop Domestication, The Harlan Symposium*; ISBN 92-9127-084-9, 1998

[6] **Diamond, Jared** *Guns,Germs and Steel*; ISBN 0-09-930278-0, 1998

[7] **Maurizio Forte, Alberto Siliotti, Foreword by Colin Renfrew** *Virtual Archaeology*; ISBN 0-500-05085-6

[8] **Anderson, William Scot** *Solving the Mystery of the Biblical Flood*; ISBN 1-40102096-8, 2001

[9] **Mithen, Steven** *After the Ice*; ISBN 0-75381-392-0, 2003

[10] **Cavalli-Sforza, Luigi Luca** *Gene, Völker und Sprachen*; ISBN 3-446-19479, 1996

[11] **Cavalli-Sforza, Menozzi, Piazza** *The history and geography of human genes*; ISBN 0-691-08750-4

[12] **Ammerman, Cavalli-Sforza** *The Neolithic Transition and the genetics of populations in Europe*; ISBN 0-691-08357-6, 1984

[13] **Cohen, M.H.** *Nonlinearity, Disorder, the Spread of Neolithic Farming and the Origin of the Indo-European Languages*; Springer, Proceedings in Physis, Vol.67, 1992

[14] **Ammerman A.J., Cavalli-Sforza L.L.** *A population model for the diffusion of early farming in Europe*; Renfrew C, editor The explanation of culture change, London: Duckworth. pp 343357, 1973

[15] **Ammerman A.J., Cavalli-Sforza L.L.** *Measuring the Rate of Spread of Early Farming in Europe*; Man, 6, 674-688, 1971

[16] **Joaquim Fort, Vicenç Méndez** *Time-Delayed Theory of the Neolithic Transition in Europe*; Physical Review Letters, Vol.82, Nr.4, 867-870, 1999

[17] **K. Davison, P.M. Dolukhanov, G.R. Sarson and A. Shunkurov** *Environmental effects on the spread of the Neolithic*; http://arxiv.org/abs/q-bio.PE/0505013

[18] **Ryan, Pitman** *Noah's Flood: The New Scientific Discoveries About the Event that Changed History*; ISBN 0-684-81052-2, 1999

[19] **Marek Zvelebil** *The agricultural transition and the origins of Neolithic society in Europe*; Documenta Praehistorica XXVIII, 8^{th} Neolithic Studies, ISSN 1408-967X, 2001

[20] **Marek Zvelebil** *Who Were We 6000 Years Ago? In Search of Prehistoric Identities*; Traces of ancestry: studies in honour of Colin Renfrew, ISBN 1-902937-25-2

[21] **Madhav Gadgil and N.V. Joshi, et. al** *PEOPLING OF INDIA*; http://ces.iisc.ernet.in/hpg/cesmg/peopling.html

A Appendices

A.1 Finding a solution for the Fisher Equation

We will now try to prove that the Fisher Equation has a traveling wave solution. First re-scale (1) for convenience by dividing by $\frac{1}{\tau}$ to get

$$\frac{\partial n\tau}{\partial t} = D\tau\nabla^2 n + n(1-n)$$

if we now define

$$t^* = \frac{t}{\tau} \qquad \text{and} \qquad x^* = x\left(\frac{1}{D\tau}\right)^{\frac{1}{2}}$$

substitute back in, drop the * notation and simplify to one dimension

$$\frac{\partial n}{\partial t} = \frac{\partial^2 n}{\partial x^2} + n(1-n) \tag{33}$$

The equation has two steady states at $n = 1$ and $n = 0$. We need a solution connecting these two states. Whatever form the solution takes, it needs to have a negative gradient to go from $n = 1$ to $n = 0$. The importance of this observation will become clear later in this derivation. If a traveling wave solution exists, then it can be written as

$$n(x,t) = U(z) \qquad \text{where} \qquad z = x - ct \qquad c = wavespeed \tag{34}$$

The wave solutions requires that

$$U \to 0 \quad \text{as} \quad z \to \infty \qquad \text{and} \qquad U \to 1 \quad \text{as} \quad z \to -\infty$$

Assume $c \geq 0$, substitute (34) into (33) and bring all terms on the left hand side to get

$$U'' + cU' + U(1-U) = 0 \tag{35}$$

It is now a eigenvalue problem to determine the values of c for which a non negative solution of (35) exists which satisfies

$$\lim_{z\to\infty} U(z) = 0 \quad \text{and} \quad \lim_{z\to-\infty} U(z) = 1$$

By introducing a new variable V we can create a first order system and can consider the system in the (U, V) phase plane.

$$U' = V \qquad \text{and} \qquad V' = -cV - U(1-U) \tag{36}$$

Equilibria when $U' = 0$ and $V' = 0 \Rightarrow V = 0$ and $U(1-U) = 0$. This implies two singular points in the phase plane, the steady states at $(0,0)$ and $(1,0)$. The earlier observation that the solution must have a negative gradient restricts a possible solution to the 4th quadrant of the phase plane. See *Figure* 30

We now carry out a Linear Stability Analysis about the two singular points.

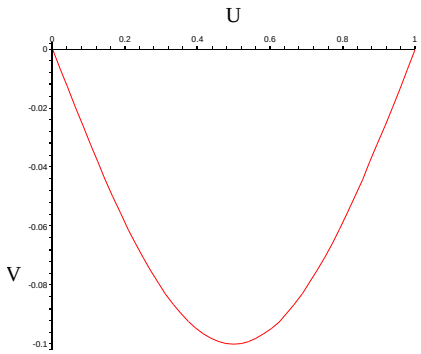

Figure 30: Possible solution in phase space

- Linearization about $(1, 0)$
  let $U = 1 + u$ and $V = v$ where $u, v \ll$ then (36) becomes

$$\begin{aligned} u' &= v \\ v' &= -cv - (1+u)(1-1-u) \approx u - cv \end{aligned} \tag{37}$$

  In matrix notation

$$\begin{pmatrix} u' \\ v' \end{pmatrix} = A \begin{pmatrix} u \\ v \end{pmatrix} \qquad A = \begin{pmatrix} 0 & 1 \\ 1 & -c \end{pmatrix}$$

  Find the eigenvalues:

$$\begin{vmatrix} -\lambda & 1 \\ 1 & -\lambda - c \end{vmatrix} = 0$$

$$\lambda^2 + c\lambda - 1 = 0$$

  Solving the quadratic

$$\lambda_{\pm} = \frac{1}{2}\left[-c \pm \sqrt{\frac{c^2}{4} + 1}\right]$$

  gives real eigenvalues with opposite sign $\Rightarrow$ a saddle point in phase space. See *Figure* 31 Let the positive eigenvalue be λ_+. From the eigenvalue equation one can obtain the eigenvector

$$-\lambda_+ u + v = 0 \qquad \rightarrow \qquad v = \lambda_+ u$$

  From (37)

$$u' = v$$

$$u' = \lambda_+ u$$

$$\frac{du}{dz} = \lambda_+ u$$

$$\int \frac{1}{u} du = \int \lambda_+ dz$$

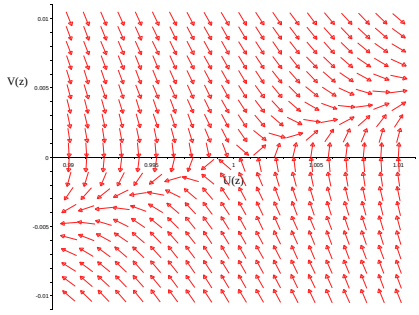

Figure 31: A stable saddle point at $(U, V) = (1, 0)$

$$u = \alpha \exp \lambda_+ z$$

Where α is an integration constant. Near the point $(1, 0)$ we have an approximate solution

$$\begin{aligned} U &= 1 + u &&= 1 + \alpha \exp \lambda_+ z \\ V &= v &&= \alpha \lambda_+ \exp \lambda_+ z \end{aligned} \tag{38}$$

Choose $\alpha < 0$ to obtain a solution pointing towards the origin. See *Figure* 32

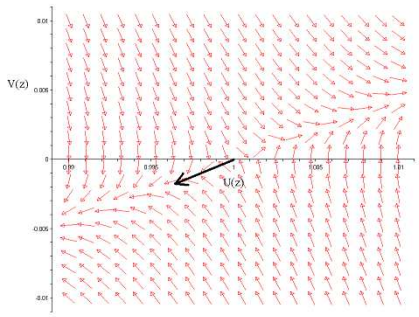

Figure 32: Choose $\alpha < 0$ to obtain a solution pointing towards the origin

- Linearization about $(0, 0)$
  let $U = u$ and $V = v$ where $u, v \ll$ then (36) becomes

$$\begin{aligned} u' &= v \\ v' &= -cv - u(1 - u) \approx -cv - u \end{aligned} \tag{39}$$

In matrix notation

$$\begin{pmatrix} u' \\ v' \end{pmatrix} = A \begin{pmatrix} u \\ v \end{pmatrix} \qquad A = \begin{pmatrix} 0 & 1 \\ -1 & -c \end{pmatrix}$$

Find the eigenvalues:

$$\begin{vmatrix} -\lambda & 1 \\ -1 & -\lambda - c \end{vmatrix} = 0$$

$$\lambda^2 + c\lambda + 1 = 0$$

Solving the quadratic

$$\lambda_{\pm} = -\frac{c}{2} \pm \sqrt{c^2 - 4}$$

this gives a stable node if $c \geq 2$ *Figure* 33 or a stable focus if $c < 2$ *Figure* 34. The second possibility of the two is ignored. A focus would mean changing the signs of U, implying negative populations which does not make sense. This suggest that

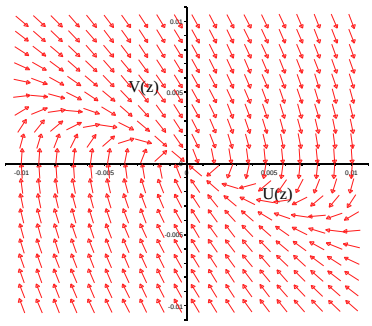

Figure 33: Stable node at $(U, V) = (0, 0)$

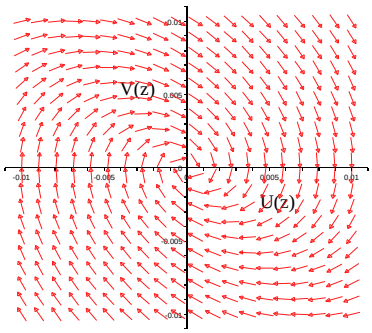

Figure 34: Spiral at $(U, V) = (0, 0)$

for any $c \geq 2$ the solutions starting at (38) tend to $(0, 0)$ as $z \to \infty$ and is non negative i.e. there is a positive traveling wave solution *Figure* 36 to the Fisher Equation(1).

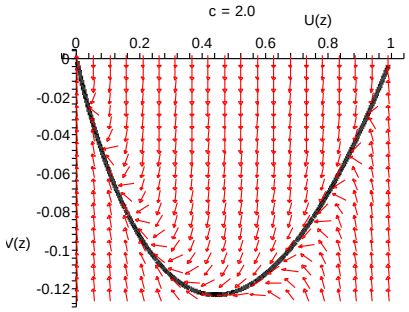

Figure 35: The full solution in phase space with $c = 2$

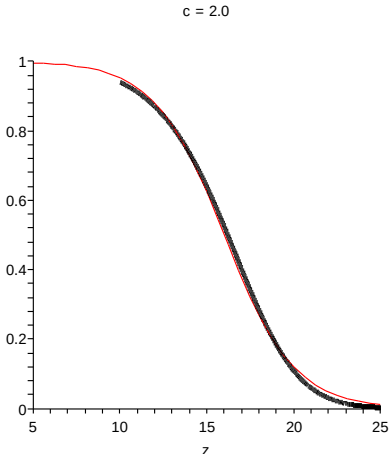

Figure 36: The full solution in real space with $c = 2$

Remembering the $c \geq 2$ is actually $\frac{dx^*}{dt^*} \geq 2$. Changing back to the original variables we obtain

$$\frac{\sqrt{\frac{1}{D\tau}}}{\frac{1}{\tau}} \frac{dx}{dt} \geq 2$$

the final expression for the wave speed:

$$\frac{dx}{dt} \geq 2\sqrt{\frac{D}{\tau}} \tag{40}$$

A.2 Solving the Diffusive Equation - Divergence of Fluxes

The divergence of fluxes is based on the saturation population N_s (which relates to the land fertility), the diffusion constant D, the size of the borders of the grid-points and the actual populations. The following model is based on the Javaman simulation by Kevin Stratford. The calculations are done in a "Typewriter"-fashion, where all the grid-points are visited in a line by line manner, starting at the top left corner $P(x_0, y_0)$ and ending at $P(x_{max}, y_{max})$. The advantage of this method is that on each grid-pint

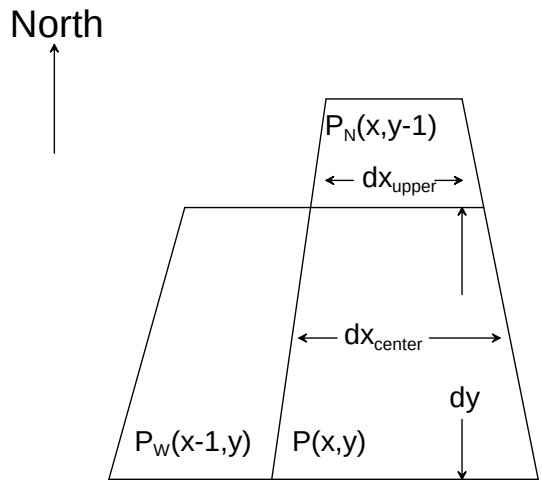

Figure 37: Divergence of Fluxes

only two boundaries i.e. north and west, need to be considered, because going through all grid-points will effectively calculate all four boundaries of each grid-point. However, this approach does not calculate boundaries for the grid-points on the edge of the array, therefore we defined to have no fluxes at the borders of the scenario arrays.
The actual calculation is done in three steps, first we pre-compute a term which is independent of the current population and therefore only needs to be computed once.

$$\begin{aligned} mask_{North}(x,y) &= D(x,y)\frac{N_s(x,y)+N_s(x,y-1)}{2}\frac{dx_{upper}}{dy} \\ mask_{West}(x,y) &= D(x,y)\frac{N_s(x,y)+N_s(x-1,y)}{2}\frac{dy}{dx_{center}} \end{aligned} \tag{41}$$

The actual fluxes across the northern and western boundaries are then related to the actual populations in the grid-points.

$$\begin{aligned} d_{fw}(x,y) &= mask_{West}(x,y)(N(x,y)-N(x-1,y)) \\ d_{fn}(x,y) &= mask_{North}(x,y)(N(x,y)-N(x,y-1)) \end{aligned} \tag{42}$$

And the final population change in a grid point due to diffusion can then be written as:

$$dN(x,y) = \frac{1}{Area(x,y)N_s(x,y)}\left[(d_{fw}(x+1,y)-d_{fw}(x,y))+(d_{fn}(x,y+1)-d_{fw}(x,y))\right] \tag{43}$$

An important point is the existence of a stability criterion for the diffusive part of the equation: $D\Delta t/\Delta x^2 < 1$. D is the diffusion constant, Δt is the discrete time step and δx is the grid size. This can be seen as a restriction that information can not travel further than Δx in one time step. Unstable behavior of the simulation can be observed if the diffusion constant D is too large.

A.3 How to use the software

Copy all the files (.java and .xyz) from the directory *code* on the CD-rom that comes with this report to a local directory of your choice. If a JAVA developer environment is installed then compile the files by typing: **javac InitialGui.java**
If you don't have a JAVA developer environment installed then you can download it from: http://java.sun.com/j2se/1.4.2/download.html Depending on which version of JAVA you have installed the above compile command might give you an error message like: *** uses or overrides a deprecated API** This message can be ignored, just type the compile command again. Then to run the program type **java -Xmx150m InitialGui**. The -Xmx command allocates 150 MByte of memory to the java virtual machine running the program, which is necessary due to the large arrays used in the simulation.
If new scenarios should be created then the files DataPrep.java and ConvertMap.java need to be compiled also. For information on how to create the maps please look to the Java Documentation of the project in the appendix or in the directory *JavaDoc* on the CD-rom for an html version.

A.4 Source Code